ELSEVIER

Fuel 80 (2001) 1809–1817

FUEL

www.fuelfirst.com

Real-time evolved gas analysis by FTIR method: an experimental study of cellulose pyrolysis

S. Li*, J. Lyons-Hart, J. Banyasz, K. Shafer

Research, Development and Engineering, Philip Morris U.S.A, P.O. Box 26583, Richmond, VA 23261, USA

Received 15 June 2000; revised 4 December 2000; accepted 4 December 2000

Abstract

A two heating zone pyrolysis system capable of a heating rate of 40°C/s and a flow rate of 70 ml/s was coupled to a rapid scanning Fourier transform infrared (FTIR) spectrometer. This fast evolved gas analysis system was applied to the study of the simultaneous evolution of low molecular weight gas phase products, such as CO, CO_2, H_2O, CH_4, C_2H_4, and CH_2O during the pyrolysis of cellulose. Different pyrolytic conditions, including heating rate, gas flow rate, and residence time, were tested to study their effects on the formation of gaseous compounds during cellulose pyrolysis. Formaldehyde and carbon monoxide formations were observed to have a strong heating rate dependence, whereas carbon dioxide formation showed little dependence with the heating rate. Efforts were made to achieve a well-controlled heating environment and sample temperature measurement. The pyrolysis of levoglucosan, a major component of tar and a primary pyrolysis product of cellulose, was also studied. Comparison of the pyrolysis products from cellulose and levoglucosan showed great similarities and provided insight into the precursors and formation mechanisms of gas phase products. This experimental method provides a technique to analyze evolved gases in real time, information on reaction mechanisms, and a method to distinguish and control primary and secondary reactions.

Keywords: Cellulose pyrolysis; Fourier transform infrared spectrometer (FTIR); Levoglucosan

1. Introduction

Cellulose pyrolysis involves a complicated set of chemical reactions that are influenced by many parameters. A number of publications have reported investigations of the overall reaction kinetics, pyrolytic decomposition pathways, and the nature and amounts of products formed [1–31]. The generally accepted mechanism for cellulose pyrolysis, based on a series of experiments by Arseneau [6], Broido [7–9], and Shafizadeh [2,3], involves an initiation reaction associated with a dramatic reduction in the degree of polymerization of the cellulose, followed by two competing reactions. At temperatures below 300°C, anhydrocellulose is produced by intramolecular water elimination, whereas at temperatures above 300°C, a rapid depolymerization or "unzipping" results in the formation of levoglucosan. The anhydrocellulose and levoglucosan further decompose to form char, permanent gases, and other volatiles during the secondary reactions. Kinetic analyses of the overall reactions have been carried out by a number of techniques, including thermogravimetric analysis (TGA), differential scanning calorimetry (DSC), pyrolysis-gas chromatography (Py-GC), pyrolysis-GC–MS, and evolved gas measurement (EGA). Most of the information reported in the literature is concerned with the global kinetics, weight loss, or heat of reaction of the overall cellulose pyrolysis process. The chemical reactions, particularly the secondary reactions, are less frequently reported because of the demands placed upon the analytical techniques to discriminate between individual compounds in a constantly changing complex matrix. The fact that many of the cellulose pyrolysis studies use a heating rate of less than 1°C/s also limits the study of products that occur at higher heating rates or temperatures.

To better understand the nature of cellulose pyrolysis under fast heating conditions, a two-reaction zone pyrolysis system was coupled to a rapid scanning Fourier transform infrared spectrometer (EGA/FTIR). By carefully controlling the pyrolytic conditions of the two-reaction zone tube furnace, specific products of the primary and secondary reactions of cellulose pyrolysis were identified. Advantages of this two reaction zone EGA/FTIR include: (1) real time measurement as the gases are formed during evolution, (2) simultaneous observation and identification of multiple gaseous compounds, (3) separation of primary and secondary

* Corresponding author.
E-mail address: san.li@pmusa.com (S. Li).

0016-2361/01/$ - see front matter
PII: S0016-2361(01)00064-3

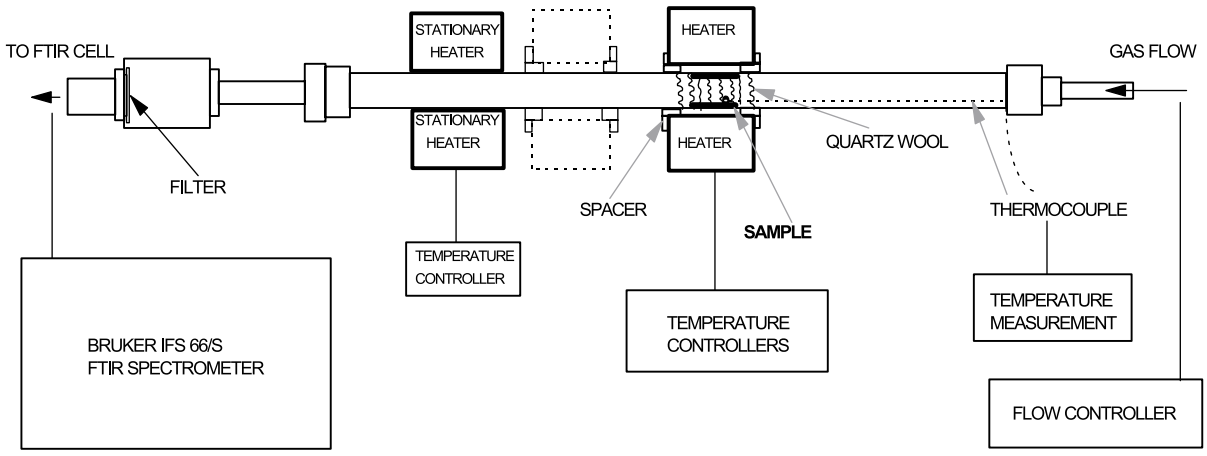

Fig. 1. Schematic diagram of the evolved gas analysis/FTIR apparatus.

reactions through the use of two reaction zones, and (4) relatively high flow rates that reduce the residence time minimizing further reactions. Application of high flow rates in this study improves temporal resolution of the formation profiles for a chosen infrared cell as a result of rapid purging the infrared flow cell. The addition of a second heater downstream at a fixed position basically created a second reaction zone where the temperature could be independently controlled from the first heating zone. This also provided a practical way to react gas phase compounds under different conditions while separating the effect of the solid phase on the gas phase evolution. In the case of cellulose pyrolysis, the primary char formed in the earlier stage of pyrolysis is left behind in the region of the primary heater, whereas the volatiles are carried away from the primary heater into the secondary heating zone where further reactions can continue. In this way, primary and secondary reactions are distinguished from each other. The effect of heating rate on the formation of formaldehyde, the pyrolysis of levoglucosan (1,6-Anhydro-β-D-glucopyranose), and the post-pyrolysis heating effect on CO and CO_2 formation will be discussed.

2. Experimental

2.1. Apparatus

A schematic of the evolved gas analysis/FTIR (EGA/FTIR) technique developed in this study is shown in Fig. 1. The apparatus consists of three major components. An FTIR spectrometer (Bruker IFS 66/s, Bruker Optics, Billerica, MA) equipped with a linear gas flow cell of 50 ml volume and 1.0 m path length (Axiom Analytical Inc., Irvine, CA), a sample chamber made of a quartz tube (7 mm i.d., 9 mm o.d., 600 mm in length) that retains the sample during pyrolysis, and a heating unit with stationary and movable heaters and appropriate temperature control devices. The movable heater is placed on a rail system and can be moved quickly and reproducibly to a desired position. The flow rates of the nitrogen carrier was controlled by a MKS 1259B mass flow controller (MKS Instruments, Inc., Burlington, MA) and measured with an Omega FMA 1818 mass flowmeter (Omega Engineering, Inc., Stamford, CT). Unless otherwise stated, the flow rate used in this study was 2100 ml/min (35 ml/s).

2.2. Sample

Twenty milligrams of Whatman No. 41 filter paper (Whatman International Limited, England), cut into rectangular strips (20 mm × 10 mm), was used as the sample without further treatment. The paper is rolled and inserted into the quartz tube to form a single layer against the wall. This single layer sample configuration is important in achieving fast and uniform heating. The position of the sample in the primary heating block was the same for all experiments. Quartz wool was used on both ends of the sample to hold it in position. In the experiments of levoglucosan, twenty milligrams of levoglucosan (1,6-Anhydro-β-D-glucopyranose) of 99.9% purity (Acros Organics, Fairlawn, NJ) was used without further purification.

2.3. Sample heating

A unique capability of this pyrolytic unit, built in-house, is the rapid heating of a relatively large sample (up to a few grams). This is achieved by using a block of stainless steel that is 38 mm × 38 mm × 135 mm and equipped with four symmetrically located cartridge heaters. The temperature of the heating block was measured by two thermocouples. Two solid state relay temperature controllers regulated the heating. The quartz tube that holds the sample is inserted through a hole of 10 mm diameter located in the center of the heating block. To achieve a homogenous heating of the sample, two spacers are embedded at the ends of the center hole so that the sample portion of the quartz tube will be in the center of the hole and not in contact with the heater body thereby eliminating conductive heating. This proves to be

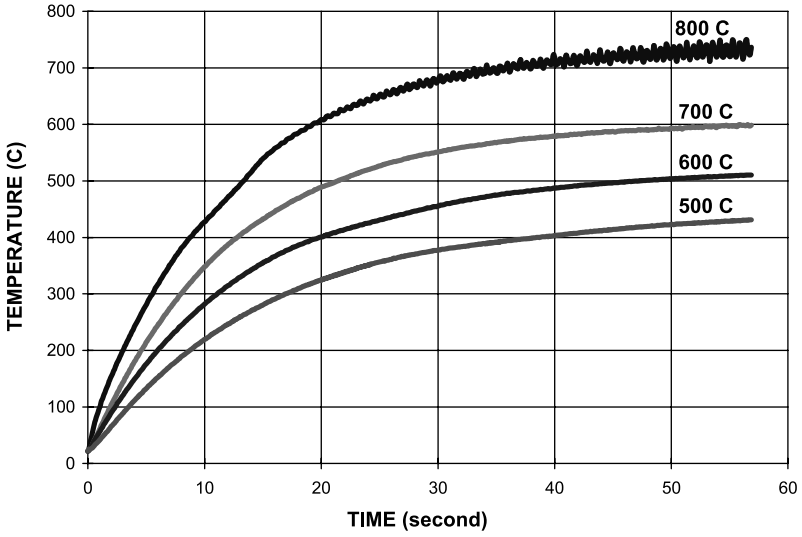

Fig. 2. Average temperature profiles of cellulose samples at four different heater temperatures.

important in achieving good reproducibility. The large thermal capacity of the block results in the capability of heating samples of a few grams without diminishing the heating rate.

At the beginning of an experiment, the sample was set at room temperature. Both the stationary heater and the movable heater were set to the desired temperatures. Once the heaters reached equilibrium the movable heater block was quickly moved to the sample position, resulting in immediate heat transfer to the sample. Heating rates were dependent, primarily, on the heater temperature.

2.4. Sample temperature measurement

The sample (Whatman filter paper) temperature is measured by two thermocouples (0.01″, type K, response time 2–4 ms, Omega Engineering, Inc., Stamford, CT) placed in contact with the inside and outside surfaces of the sample. Average temperature of the sample was determined from the outside and inside surface temperatures. Calculations with temperatures measured at the inside and outside surface of the samples showed a 10% difference in activation energy, which is not significant considering other possible sources of errors.

A Data Translation board using LABTECH Notebook software (Laboratory Technologies Corporation, Andover, MA) recorded the temperature-time profiles. The sampling frequency was set to match the infrared spectrometer scanning frequency, 12.42 Hz corresponding to one temperature measurement every 80.5 ms in the current experiment. Fig. 2 displays the temperature profiles at different heating rates (heater temperatures). The measured temperature profiles of the samples can be described by an exponential equation:

$$T(t) = T_0 + (T_\infty - T_0)(1 - \exp(-t/\tau)) \quad (1)$$

where T_0 and T_∞ refer to the initial and final temperatures, τ the time constant for the temperature rise, and t is the time. Table 1 lists, among other parameters, T_0, T_∞, and τ derived from the temperature profiles from cellulose pyrolysis.

When quartz wool was used as the sample inside the tube furnace, the temperature was determined by three thermocouples placed at different positions across the sample. The temperature profiles obtained were reproducible with a temperature gradient of less than 30°C across the sample when the heater was set at 800°C (the fastest heating rate in this study). Smaller temperature gradients were observed when slower heating rates were used (lower heater temperatures).

The flow rate through the furnace tube (which impacts the reaction kinetics) is affected by changes in the carrier gas temperature and the evolution volume of pyrolytic gases. In order to assess the magnitude of such perturbations of flow, the rate was monitored during the course of the pyrolysis process. No significant change in the flow rate was observed during pyrolysis.

2.5. Second heating zone

Another feature of the current fast EGA/FTIR technique is the addition of a stationary heater placed downstream just before the gas flows into the IR cell creating a second reaction zone. This allowed one to study the effect of temperature on further reaction of primary pyrolysis products. No condensation was observed between the two heated zones, indicating that most primary pyrolysis products generated in the first heating zone pass into the second heating zone. The temperature of this intermediate zone between the two heaters is in the range of 200–400°C, depending on the primary heater temperature settings. The temperature and residence time was precisely controlled providing an experimental way to distinguish primary and secondary reactions.

Table 1
Temperature data and formation of CH_2O, CO, and CO_2 from cellulose pyrolysis

Heater temperature (°C)	Compounds	T_0 (°C)[a]	T_∞ (°C)[a]	T_{max} (°C)[b]	τ (s)[a]	Integrated Area[c]
800	CH_2O	22	733	438 (11)	11.8	1.53 (0.04)
	CO			440 (19)		0.435 (0.02)
	CO_2			415 (18)		1.12 (0.04)
750	CH_2O	22	694	427 (10)	13.4	1.29 (0.09)
	CO			443 (14)		0.354 (0.02)
	CO_2			414 (18)		1.074 (0.07)
700	CH_2O	22	608	436 (3)	13.7	1.19 (0.05)
	CO			439 (6)		0.338 (0.05)
	CO_2			414 (20)		1.19 (0.07)
650	CH_2O	23	585	422 (5)	14.1	1.16 (0.05)
	CO			430 (5)		0.322 (0.02)
	CO_2			400 (8)		1.16 (0.08)
600	CH_2O	22	518	409 (3)	14.4	1.12 (0.08)
	CO			417 (4)		0.307 (0.02)
	CO_2			393 (3)		1.24 (0.04)
550	CH_2O	23	494	420 (5)	15.0	0.969 (0.06)
	CO			427 (7)		0.256 (0.03)
	CO_2			405 (12)		1.13 (0.04)
525	CH_2O	23	452	400 (6)	15.2	0.959 (0.08)
	CO			402 (8)		0.333 (0.05)
	CO_2			392 (6)		1.30 (0.08)
500	CH_2O	23	446	392 (3)	16.4	0.964 (0.05)
	CO			388 (5)		0.217 (0.03)
	CO_2			379 (4)		1.21 (0.07)
475	CH_2O	22	412	383 (3)	16.9	0.872 (0.04)
	CO			379 (2)		0.276 (0.08)
	CO_2			372 (5)		1.24 (0.12)
450	CH_2O	23	383	370 (2)	17.1	0.870 (0.14)
	CO			368 (3)		0.231 (0.03)
	CO_2			362 (2)		1.25 (0.14)

[a] From $T(t) = T_0(T_\infty - T_0)(1 - \exp(-t/\tau))$, where the subscripts 0 and ∞ refer to the initial and final temperatures of the samples and τ is the time constant for the temperature rise. T_0, T_∞ and τ are average values from measured temperature profiles inside and outside the samples.
[b] Measured temperature when maximum formation rate is observed. Averages of the temperatures measured at the inside and outside of the samples were listed in this table. The experimental uncertainties are indicated in parentheses.
[c] Integrated area under the formation profile. The experimental uncertainties are indicated in parentheses.

2.6. FTIR spectrometer

In order to measure the formation profiles of gaseous compounds in real time during a fast heating process, the FTIR spectrometer is required to have a fast scanning velocity. The Bruker IFS 66/s FTIR spectrometer is set to repetitively collect 500 interferograms at a resolution of 1 wavenumber and sampling frequency of 200 kHz (i.e. 0.0805 s/scan, 40 s total for an experiment). At a nitrogen flow rate of 2100 ml/min, a cell volume of 50 ml, and a 1.0 m path length, the time required to completely displace one cell volume is 1.43 s, or every 17.8 scans. Ideally, the IR cell would have a minimum volume and a maximum path length. A narrow range liquid nitrogen cooled mercury cadmium telluride (MCT) detector was used to cover the spectral range of 3800–750 cm^{-1}. Calibration curves were obtained for several standard gas samples. The interferograms were collected during the pyrolysis and post-processed to obtain the absorption spectra and gas formation profiles. Two fresh Cambridge pads (15.9 mm in diameter) were placed at the entrance of the gas flow cell in each analysis to filter out the particulate matter. The flow cell was heated to 180°C during the experiment to prevent condensation of gases on the KBr windows and on the cell wall.

2.7. Procedures

Both the stationary heater and movable heater were set at the desired temperatures with the movable heater positioned on the rail away from the sample. It should be noted that all the experimental results in our kinetic studies [32,33] were obtained by using only the movable sample heater, keeping the secondary heater at room temperature. The nitrogen gas flow was measured by a flow meter, and the infrared

spectrum and temperature measurements were started simultaneously. After about three seconds, the heater was positioned over the sample. The heater block was moved in the same time frame with each measurement so that the heating rates experienced by the samples were reproducible. The sample temperature is measured and monitored by thermocouples throughout the pyrolysis process. It should be noted that the "true" sample temperature is rather difficult to obtain during a dynamic process, especially at a fast heating rate. The measured temperatures in this study were averages of at least five experimental runs, and should closely represent the sample temperatures. Post data processing included Fourier transforming interferograms to single beam spectra, calculating absorption spectra using the first ten single beam spectra co-added at the beginning of the experiment as the background, and obtaining the gas evolution profiles from the absorption spectra. A further reduction in flow cell volume or increase in the flow rate through the addition of a make-up gas was possible to further increase the temporal resolution, however, at the expense of reduced infrared absorbance or signal.

3. Results and discussion

As described in Section 2, the infrared spectra and the temperature measurements were performed simultaneously. As the gaseous compounds were generated during the heating process, they were continuously flushed through the infrared cell and measured every 80 ms. Formaldehyde, CO, CO_2, and hydroxyacetaldehyde monitored in this study were shown to have linear absorption-concentration relationships. The gas evolution profile for each molecule was constructed from the infrared absorption and time or temperature. From the gas evolution profiles, information such as the starting formation temperature, the completion temperature, the maximum formation temperature, as well as the sequence of formation of products was obtained. As discussed earlier, average values of several temperature measurements were taken as representative of the temperature of the sample. Table 1 summarized the temperature data, including the initial and final temperatures of the sample, the time constant of temperature rise, the maximum formation temperature, and integrated areas of the evolution profiles which are directly related to the amount of compounds formed at the different heating rates. The evolution profiles of about ten compounds, including formaldehyde, carbon monoxide, carbon dioxide, water, methane, ethylene, methanol, hydroxyacetaldehyde, formic acid, and carbonyl group compounds, were monitored simultaneously during the pyrolysis of cellulose, however, only three compounds, formaldehyde, carbon monoxide, and carbon dioxide are reported in this study (Table 1). In this table, differences in compounds generated at different temperatures indicate different precursors and reaction routes, and different heating rate dependencies. Formaldehyde and carbon monoxide formations were observed to have a strong heating rate dependence, whereas carbon dioxide formation had little dependence with the heating rate. The carbon dioxide maximum formation temperatures are also lower than that of formaldehyde and carbon monoxide, as indicated in Table 1. Further information on the reaction kinetics and mechanism can be derived from the data listed in Table 1, and will be discussed in separate papers [32,33].

3.1. Formaldehyde formation

The absorbance of formaldehyde was determined at different heating rates to examine their effect in cellulose pyrolysis. Fig. 3 shows the formaldehyde formation profiles at different heating rates achieved by setting the heater at different temperatures. A formation profile is constructed by choosing a unique absorption band for a particular compound and measuring its intensity change throughout the pyrolysis. The absorbance of that band is then plotted over time. The areas under the profiles were integrated and used as an indication of the amount of gas formed in the pyrolysis. The absorption band of formaldehyde at

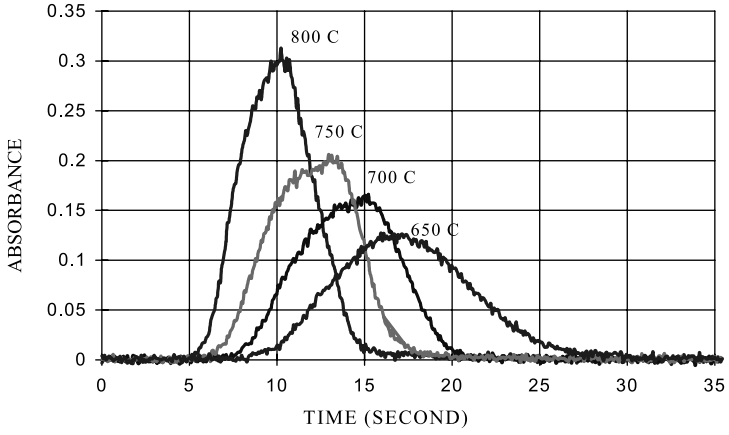

Fig. 3. Formaldehyde formation profiles from cellulose pyrolysis at different heating rates. Note that the time axis can be readily converted to temperatures.

2780.9 cm^{-1} resulting from the rotational structure of the C–H stretching was used to construct the formation profiles of formaldehyde. Since the sample temperatures are recorded at the same time, temperatures corresponding to the maximum formation rates at different heating conditions can be determined. The temperature of maximum formation, the amount of product formed, as well as the start and end of product formation are derived from the formation profile. It is clearly seen that both the maximum temperature of formation and the amount of formaldehyde formed are dependent on the sample-heating rate. As the heater temperature increased from 450 to 800°C, the heating rate and the amount of formaldehyde increased. The T_{max} shifted to higher temperature when the heating rate is increased. The increased formaldehyde formation at higher heating rate provides evidence for the shifting of cellulose pyrolysis pathway to depolymerization or "unzipping" at higher heating rate and temperature. A more in-depth analysis of the data in the determination of a kinetic mechanism of cellulose pyrolysis will be presented elsewhere [32,33].

The amounts of carbon monoxide and carbonyl containing compounds (as monitored by the carbonyl group frequency at 1760.0 cm^{-1}) increased with increasing heating rate, whereas CO_2 and H_2O formation decreased with increasing heating rate. These different heating rate dependencies of different compound formation are indicative of different mechanisms of formation. A more detailed understanding of the formation mechanisms of these gases may provide further insight into cellulose pyrolysis.

Pyrolysis experiments at 4200, 2100, 1050 and 525 ml/min were performed to examine the residence time effect on formaldehyde formation. The residence time of the vapor phase in the heated zone was varied by either changing the flow rate or by placing the sample at different positions in the heater. At a flow rate of 2100 ml/min, the residence time of the vapor phase in the heated zone was varied from 0.03 to 0.12 s by placing the sample at about one inch from the exit or entrance of the heating zone, respectively. Slower flow or longer residence times produced more formaldehyde. This observation is consistent with the nature of formaldehyde formation from secondary reactions, as proposed recently in a kinetic model by us [32,33] as well as in cellulose pyrolysis literature for small organic molecule formations in general. Slower flow or longer residence times in the heated zone would simply allow more intermediates or precursors to decompose to form more formaldehyde.

Studies of flame-retardant treatment of cellulose as well as the mechanism of their effects on cellulose pyrolysis have been extensively reported in the literature. Addition of different inorganic salts can significantly alter the formation of formaldehyde as well as other gas phase products of cellulose pyrolysis. The inorganic salts act as either a tar promoter or char promoter, which directly affects the final pyrolysis products. A number of inorganic salt additives have been examined in this study. When cellulose samples were treated with $FeCl_3$, the formation of formaldehyde, CO, and CO_2 were increased. On the other hand, addition of $KHCO_3$ into cellulose decreased formaldehyde formation, while increasing CO and CO_2. It was observed that the addition of $FeCl_3$ increased the tar yield whereas the addition of $KHCO_3$ decreased the tar yield in cellulose pyrolysis. The reduced tar yield results in decreased formaldehyde. When the cellulose sample was heated at 270°C under a nitrogen environment for 15 h, then cooled down to room temperature and pyrolyzed as usual, formaldehyde yield was found to be reduced by about 80%. The tar yield was lowered, too. Most likely the low temperature heating of cellulose produced more char thereby decreasing the formation of tar, a precursor of formaldehyde formation.

3.2. Pyrolysis of 1,6-Anhydro-β-D-glucopyranose

In the initial degradation of cellulose pyrolysis, tar is one of the primary products from cellulose decomposition of which levoglucosan (1,6-anhydro-β-D-glucopyranose) is a major component. Levoglucosan formation from cellulose pyrolysis was proposed by scission of the 1,4 glucosidic linkage in the cellulose molecule, followed by intramolecular rearrangement of the monomer units. The purity and physical properties of cellulose as well as the experimental conditions appear to have a significant effect on the yield of levoglucosan formation. Shafizadeh et al. confirmed that levoglucosan can be obtained in yields from 20 to 60% by weight in their vacuum pyrolysis study of various cellulose samples [5]. While vacuum pyrolysis of cellulose results in rapid distillation of levoglucosan, under normal pyrolysis conditions, levoglucosan can further decompose to produce low molecular weight molecules and so reduce the overall yield of levoglucosan. In order to have a better understanding of the origins of the gas phase compounds, it was of interest to compare the products from levoglucosan and cellulose pyrolysis. In this study, levoglucosan was pyrolyzed with the two heating zone furnace. When the second heater was set at room temperature, 25°C, only a small amount of formaldehyde, CO, CO_2, water, and some carbonyl compounds were formed because levoglucosan is known to be easily volatilized. Vacuum pyrolysis, which facilitates the removal of reaction products, has resulted in the recovery of a rather large portion of intact levoglucosan. When the second heater was set at 800°C, however, gas phase products were significantly increased. Formaldehyde yield was increased by a factor of more than ten. This indicates that gas phase levoglucosan further decomposed in the second heater at the higher temperature. Fig. 4 compares the pyrolysis products from cellulose and levoglucosan under the same experimental conditions. Here the cellulose and levoglucosan were pyrolyzed at 800°C by the first heater, and the pyrolysis products then passed through the second heater also set at 800°C. The residence time inside the secondary heater was about 120 ms. Indeed, very similar infrared spectra and gas phase products were found in these two experiments. The spectral regions of 3200–2700 cm^{-1},

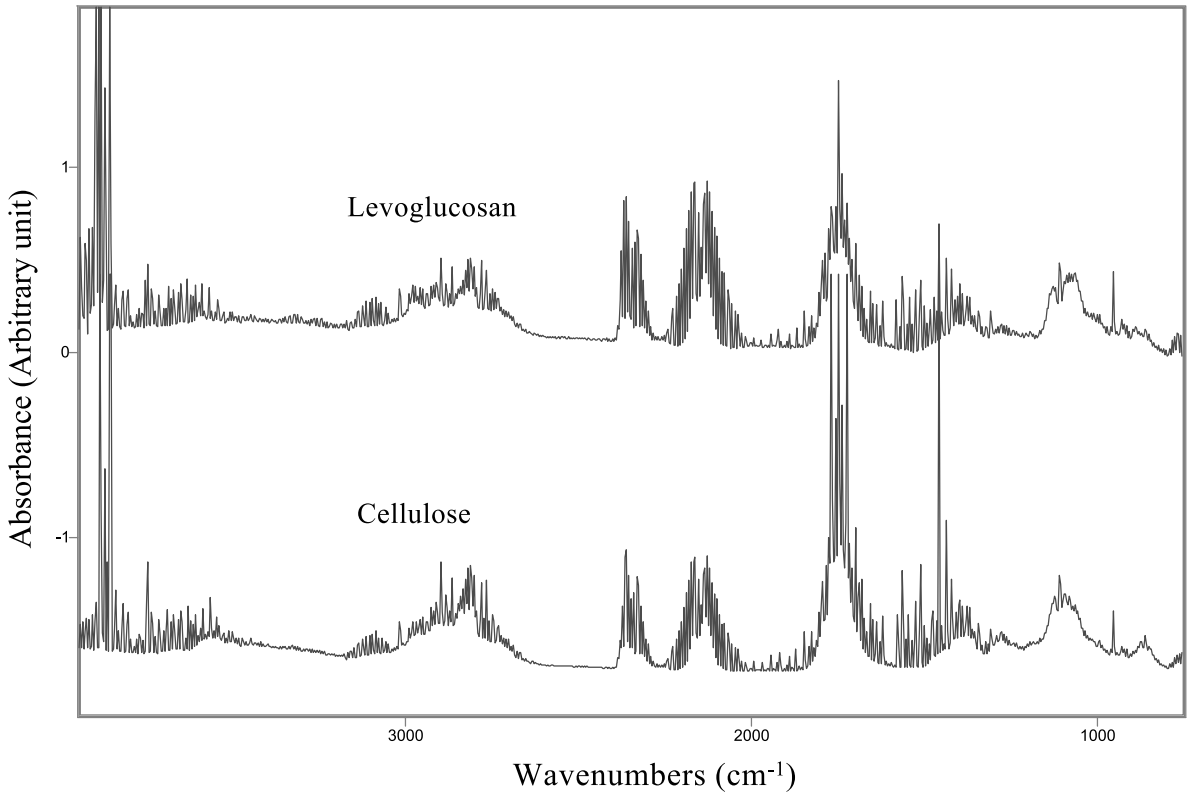

Fig. 4. Comparison of gas phase infrared absorption spectra from pyrolysis of cellulose and Levoglucosan. Same experimental conditions were applied in the two runs.

where methane, formaldehyde, and acetaldehyde absorb, are almost identical in both levoglucosan and cellulose pyrolysis. The CO_2 and CO regions (2400–2000 cm^{-1}) are also very similar in both cases. The similarities between pyrolysis of cellulose and levoglucosan support our proposed formation mechanism on formaldehyde formation. An important difference between levoglucosan and cellulose pyrolysis is the observation of hydroxyacetaldehyde absorption at 860.4 cm^{-1} in the cellulose experiment. This hydroxyacetaldehyde absorption was absent in levoglucosan experiment.

Shafizadeh had proposed a reaction scheme to explain the origin of hydroxyacetaldehyde [1]. In his mechanism, levoglucosan was first produced in the pyrolysis of cellulose, which yields glucose and then undergoes C_2–C_3 scission to form hydroxyacetaldehyde and a tetrose that then degrades further: cellulose → levoglucosan → glucose → hydroxyacetaldehyde + tetrose. Piskorz, et al., used the similar reaction mechanism to explain the formation of hydroxyacetaldehyde in their studies of rapid cellulose pyrolysis [19]. Richards [23], in a study of vacuum pyrolysis of cellulose at 350°C, argued that this mechanism is very unlikely based on the fact that conditions which increase levoglucosan yield cause a dramatic decrease in hydroxyacetaldehyde yield. Richards proposed that the hydroxyacetaldehyde formation must involve diversion of reaction channels prior to the formation of levoglucosan. In our experiments on pyrolysis of levoglucosan, no detectable hydroxyacetaldehyde was observed, indicating that levoglucosan is not a major precursor of hydroxyacetaldehyde in cellulose pyrolysis.

3.3. CO and CO_2 formation: post-pyrolysis heating effect

CO and CO_2 are both observed as cellulose pyrolysis products. While they can be formed from either primary or secondary reactions, there are additional formation routes during the pyrolysis process where CO and CO_2 can be produced. Formaldehyde, a secondary product from the decomposition of tar (levoglucosan), can thermally decompose to produce H_2 and CO at around 550°C. Several experiments were performed using the same heating rate in the primary pyrolysis zone while applying a different heating rate at the second heating zone. The use of a secondary heater provided a heated zone for secondary reactions to continue after the primary reaction products leave the first pyrolysis zone. Fig. 5 shows the CO and CO_2 formation at different secondary heater temperatures (the primary heater temperature was fixed at 800°C). The rotational structure at 2055.3 cm^{-1} of CO vibration and the band at 2251.6 cm^{-1} of the ν_3 mode of CO_2 vibration were used to monitor the formation of the two gases. When the second heater temperature was set lower than 500°C, the secondary-heating zone did not significantly affect the CO and CO_2

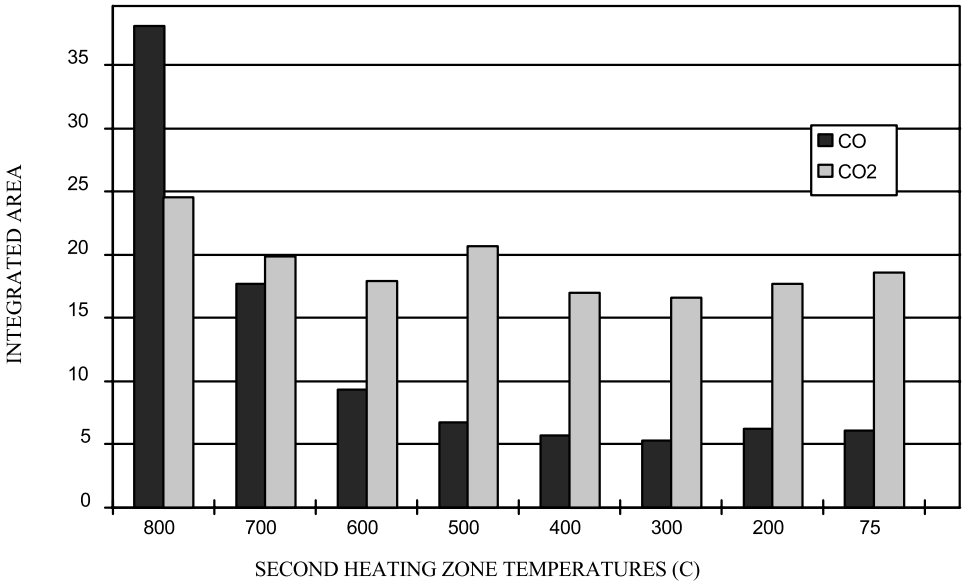

Fig. 5. Comparison of gas phase CO and CO_2 formation from cellulose pyrolysis. The primary heater was set at 800°C and the second heater was set at different temperatures.

output. When the second heater temperature was set at higher than 500°C, CO formation from cellulose pyrolysis was found to be highly dependent on the temperature set at the second zone, while CO_2 yields were only slightly affected by the additional heating. The dependence of CO formation on temperature is well known in the literature [17,20], and the yield of CO does correlate to the pyrolysis temperature. The post-pyrolysis heating effect on CO formation is of interest since it provides additional information on the formation sources of CO, such as further cracking of aldehydes. Although it is difficult to completely distinguish the primary reaction products from that of secondary reactions, the two heating zone experiment as performed does indicate that a large portion of CO is formed by the secondary reactions, i.e., the decomposition of the primary volatile products. Most CO_2 is produced in the primary reaction or early stage of cellulose pyrolysis under the fast heating condition. CO and CO_2 also have different maximum formation temperatures as seen in Table 1, with T_{max} slightly lower for CO_2. Again this may result from CO and CO_2 forming from different precursors and at different stages during the pyrolysis. Further correlation of CO and CO_2 with other gases might reveal more insights into the formation and decomposition of cellulose pyrolysis products.

4. Summary

The real time evolved gas analysis/Fourier Transform infrared (EGA/FTIR) method developed in this study was successfully applied to study the gas phase compound evolution of cellulose pyrolysis. The effects of different pyrolytic conditions, such as heating rate, gas flow rate, and the residence time of the vapor phase in the heated zone, on cellulose pyrolysis products were demonstrated. It was found that the final gaseous compounds were significantly affected by the pyrolytic conditions applied. Cellulose samples treated with different additives were found to have different yields of formaldehyde, CO, and CO_2. Both the maximum temperature of formaldehyde formation and the amount of formaldehyde formed were dependent on the sample-heating rate. Levoglucosan (1,6-anhydro-β-D-glucopyranose), a major component of cellulose tar, was found to be the major precursor of formaldehyde formation. This was supported by experimental results on levoglucosan pyrolysis. By this technique, evolved gases were analyzed at fast heating rates and information regarding formation profiles and reaction mechanisms was obtained. In the two heating zone experiments, CO formation was found to be highly dependent on the temperature set at the second zone, while CO_2 was only slightly affected by the additional heating, indicating further decomposition of vapor products to produce CO. The two heating zone furnace experiments provide further information on primary and secondary reactions of cellulose pyrolysis.

Acknowledgements

The authors would like to acknowledge Dr X. Liang for fruitful discussions and Mr D. O'Con for machinery support during this work.

References

[1] Shafizadeh F. J Anal Appl Pyrolysis 1982;3:283.
[2] Shafizadeh F, Bradbury AGW. J Appl Polym Sci 1979;23:1431.

[3] Bradbury AGW, Sakai Y, Shafizadeh F. J Appl Polym Sci 1979;23:3271.
[4] Shafizadeh F, Lai Z. J Org Chem 1972;37:278.
[5] Shafizadeh F, Furneaux RH, Cochran TG, Scholl JP, Sakai Y. J Appl Polym Sci 1979;23:3525.
[6] Arseneau DF. Can J Chem 1971;49:632.
[7] Broido A, Evett M, Hodge CC. Carbohydr Res 1975;44:267.
[8] Broido A, Nelson MA. Combust Flame 1975;24:263.
[9] Broido A, Weinstein M. Combust Sci Technol 1970;1:279.
[10] Tang WK, Neill WK. J Polym Sci 1964;6:65.
[11] Golova OP. Russ Chem Rev 1975;44:687.
[12] Golova OP, Krylova RG. Dokl Akad Nauk SSSR 1957;116:419.
[13] Antal Jr. MJ. Biomass pyrolysis: a review of the literature. In: Boer KW, Duffield JA, editors. Advances in Solar Energy, Part I – carbohydrate pyrolysis. New York: Solar Energy Society, 1982. p. 61.
[14] Antal Jr. MJ. Ind Eng Chem Prod Res Dev 1982;22:366.
[15] Mok WS-L, Antal MJ. Thermochim Acta 1983;68:165.
[16] Cullis CF, Hirschler MM, Townsend RP, Visanuvimol V. Combust Flame 1983;49:235.
[17] Baker RR. Thermal J Anal 1975;8:163.
[18] Hajaligol MR, Howard JB, Longwell JP, Peters WA. Ind Eng Chem Proc Des Dev 1982;21:457.
[19] Piskorz J, Radlein D, Scott DS. J Anal Appl Pyrolysis 1986;9:121.
[20] Radlein D, Piskorz J, Scott DS. J Anal Appl Pyrolysis 1991;19:41.
[21] Funazukuri T, Hudgins RR, Silveston PL. J Anal Appl Pyrolysis 1987;10:225.
[22] Milosavljevic I, Oja V, Suuberg EM. Ind Eng Chem Res 1996;35:653.
[23] Richards GF. J Anal Appl Pyrolysis 1987;10:251.
[24] Caballero JA, Font R, Marcilla A. J Anal Appl Pyrolysis 1996;38:131.
[25] Izawa K, Matsukura M, Ishizu Y. Agric Biol Chem 1990;54:957.
[26] Lephardt JO, Fenner RA. Appl Spectrosc 1980;34:174.
[27] Boutin O, Ferrer M, Lede J. J Anal Appl Pyrolysis 1998;47:13.
[28] Burton HR, Childs Jr. G. Beitrage zur Tabakforschung 1977;9:45.
[29] Ericsson IT. Chromatographia 1973;6:353.
[30] Graham RG, Bergougnou MA, Freel BA. Biomass Bioenergy 1994;6:33.
[31] Solomon PR, Hamblen DG, Carangelo RM. In: Voorhees KJ, editor. Analytical pyrolysis: Techniques and applications. London: Butterworths, 1984.
[32] Banyasz J, Li S, Lyons-Hart J, Shafer K. J Anal Appl Pyrolysis 2001;57:223.
[33] Banyasz J, Li S, Lyons-Hart J, Shafer K. Submitted for publication.